J. Phys. B: At. Mol. Opt. Phys. 27 (1994) 2613-2624. Printed in the UK

Differential cross sections for electron impact excitation of the $C\,^3\Pi_u$, $E\,^3\Sigma_g^+$ and $a''\,^1\Sigma_g^+$ states of N_2

Mariusz Zubek† and George C King‡

† Department of Molecular Physics, Technical University, 80-952 Gdańsk, Poland
‡ Department of Physics, Schuster Laboratory, University of Manchester, Manchester M13 9PL, UK

Received 8 March 1994

Abstract. Differential cross sections for electron impact excitation of the optically forbidden $C\,^3\Pi_u$, $E\,^3\Sigma_g^+$ and $a''\,^1\Sigma_g^+$ states of N_2 have been measured at incident energies of 17.5 and 20 eV and over the angular range 10 to 100°. Cross sections for vibrational and electronic transitions have been obtained. Integral electronic cross sections for the $C\,^3\Pi_u$ and $E\,^3\Sigma_g^+$ states have also been determined. The present results are compared with previous experimental and theoretical studies.

1. Introduction

The differential cross sections for electron impact excitation of atomic and molecular states provide valuable information about their excitation mechanisms and also about the symmetry of the states. When integrated over the whole angular range they give the integral excitation cross sections which can be used to model gaseous discharges (see Loureiro and Ferreira (1989) for the case of N_2) and to understand physical phenomena in the upper atmosphere. For example, observation of the volume emission rate of the second positive, $C\,^3\Pi_u$–$B\,^3\Pi_g$ (0, 0) band of N_2 is an accepted method of investigating the ambient photoelectron energy distributions in the thermosphere in the 100–200 km altitude range (Hernandez *et al* 1983). Despite their importance, however, relatively few experimental or theoretical studies have been made of inelastic cross sections in molecules for values of incident electron energy below about 25 eV (see review by Trajmar and Cartwright 1984). This is due, in part, to the inherent difficulties in both the experimental and computational techniques.

Differential electronic cross sections for the optically forbidden $C\,^3\Pi_u$, $E\,^3\Sigma_g^+$ and $a''\,^1\Sigma_g^+$ states of N_2 (as well as for seven others) have been measured by Cartwright *et al* (1977a). These authors analysed electron energy loss spectra measured at a number of values of scattering angle and incident electron energy from 15 to 50 eV using the least squares fitting program. Subsequently these authors renormalized their inelastic data using newer values of the elastic cross section (Trajmar *et al* 1983). More recently, these measurements have been repeated by Brunger and Teubner (1990) who used the same experimental techniques and computer analysis procedure. These new results for the $C\,^3\Pi_u$ and $E\,^3\Sigma_g^+$ states disagree significantly with the measurements of Trajmar *et al* both in the magnitude and angular dependence of the cross sections. For example,

0953-4075/94/122613+12$19.50

the $C\,^3\Pi_u$ cross sections at 20 eV incident energy and at forward scattering angles differ by a factor of 2 and show quite different angular behaviour. Also at 17.5 eV, the $E\,^3\Sigma_g^+$ cross section of Brunger and Teubner shows a much faster decrease with angle than do the results of Trajmar *et al*, displaying a minimum at about 75° (see figure 4). Apart from these two, the most comprehensive measurements for the $v=0$ level of the $C\,^3\Pi_u$ state have been reported by Finn and Doering (1975) at 20, 40 and 100 eV incident energy, while Furlan *et al* (1990) have measured the $C\,^3\Pi_u$, $E\,^3\Sigma_g^+$ and $a''\,^1\Sigma_g^+$ cross sections at 35 eV relative to the optically allowed states of Π_u and Σ_u^+ symmetries that lie between 12.45 and 13 eV.

On the theoretical side, the differential cross sections of the $C\,^3\Pi_u$ and $E\,^3\Sigma_g^+$ states have been calculated by Cartwright *et al* (1977a) within the Born–Ochkur–Rudge approximation and by Fliflet *et al* (1979) who used the distorted-wave method. In both methods the Born–Oppenheimer and Franck–Condon approximations were applied. The distorted-wave calculations reproduce the angular dependence of the cross sections observed experimentally, but overestimate their magnitude by factors of between 2 and 4. No calculations of the $a''\,^1\Sigma_g^+$ cross sections have been reported.

In the present work differential cross sections for excitation of the $C\,^3\Pi_u$, $E\,^3\Sigma_g^+$ and $a''\,^1\Sigma_g^+$ of N_2 have been measured at incident energies of 17.5 and 20 eV and over the angular range 10 to 100°. These involve the $v=0$, 1, 2 and 3 vibrational levels of the $C\,^3\Pi_u$ state, $v=0$ level of the $E\,^3\Sigma_g^+$ state and $v=0$ and 1 of the $a''\,^1\Sigma_g^+$ state. It was observed that the vibrational cross sections of the $C\,^3\Pi_u$ and $a''\,^1\Sigma_g^+$ states show significant non-Franck–Condon behaviour for both incident energies. The electronic cross sections were therefore determined by summing over the measured individual vibrational levels and including an estimated contribution from higher unobserved levels. These measurements have been undertaken to resolve the discrepancies in the existing differential cross section data and to provide additional information for the establishment of reliable integral cross sections, especially for the $C\,^3\Pi_u$ state. The magnitude of the $C\,^3\Pi_u$ integral cross section obtained by Cartwright *et al* (1977b) and Trajmar *et al* (1983) was recently brought into question when it was used in model calculations of electron transport parameters that are measured in swarm experiments (Tagashira *et al* 1980, Phelps and Pitchford 1985, and see also comment in reference 15 of Jelenkovic and Phelps 1987). On the other hand Zubek (1994) obtained cross section data for the $C\,^3\Pi_u$ state in the near-threshold region up to 17.5 eV from measurements of the second positive band emission that agreed with the results of Trajmar *et al* to within better than 25%. The present measurements are also intended to meet a need that has been generated by recent and significant advances in the calculations of the cross sections. The *R*-matrix method and Schwinger multichannel and complex Kohn variational methods are now being applied with much success to the inelastic scattering of electrons by molecules and there is the need for reliable data with which to test the theoretical approaches.

2. Apparatus and experimental details

2.1. Apparatus

The main elements of the apparatus are an electron monochromator, an analyser for the scattered electrons and a molecular beam source. The apparatus also includes a detector for molecules in metastable states which is placed above the scattering region.

The electron monochromator is based on a hemispherical deflector analyser of mean radius 50 mm and has been described in detail by Brunt *et al* (1977). Of particular note is the lens system between deflector analyser exit and the interaction region which consists of a combination of two triple-element aperture lenses and two defining apertures placed between them. The focusing of the lenses is adjusted so that an exchange of window and pupil is obtained and this allows a zero beam angle of the electron beam at the scattering region minimizing the angular divergence of the beam. This combination of lenses also provides the required range of incident electron energy (5–30 eV) whilst maintaining a fairly constant beam current which is typically 1 nA. This beam current is monitored by a Faraday cup that is placed on the incident beam axis behind the interaction region. The energy spread of the incident beam in the measurements was typically 40 meV.

The scattered electron analyser uses a hemispherical deflector with a mean radius of 20 mm and has been described by Warner *et al* (1986). A single three-element cylinder lens focuses scattered electrons onto the entrance aperture of the deflector. A defining aperture is placed at the front of the cylinder lens at a distance of 25 mm from the scattering region to limit the acceptance angle of the analyser which remains constant over the scattered electron energy range. The analyser rotates about the axis of the molecular beam through the angular range $-10°$ to $100°$ with respect to the incident beam direction. Electrons transmitted by the analyser are detected by a single channel electron multiplier. The energy resolution of the analyser was typically 40 meV giving an overall spectrometer resolution of approximately 60 meV when operating in the energy loss mode.

The molecular beam emanates from a tube of internal diameter 1.0 mm and length 12 mm which is placed at 90° with respect to the incident beam axis. The driving pressure of N_2 behind the tube was typically 80 Pa and the background pressure in the vacuum chamber was maintained at 6×10^{-3} Pa. The interaction region is surrounded by a high transparency mesh which serves to exclude extraneous electrostatic fields. This mesh has entry and exit holes for the incident and scattered electrons.

The metastable detector consists of a channel electron multiplier with a conical input placed behind suitably biased grids to exclude scattered electrons and positive ions. The detector is approximately 25 mm from the gas tube and is positioned to intercept most of the metastable molecules produced. The metastable excitation signal served to monitor continuously the experimental conditions in the interaction region (e.g. incident beam current and target pressure). The observed variations of the metastable counting rate which were less than 10% allowed corrections to be applied to the scattered electron intensities.

2.2. Experimental procedure

The differential cross sections of the states of interest were determined from energy loss spectra obtained over the energy loss range from 10.8 to 12.7 eV. These spectra were measured for various values of scattering angle, θ, over the range 10 to 100° and for values of incident electron energy 17.5 and 20 eV. An example of an energy loss spectrum obtained at an energy of 17.5 eV and an angle of 30° is shown in figure 1(*a*). At an overall energy resolution of the spectrometer of 60 meV all the states of interest apart from the $v = 1$ level of a'' $^1\Sigma_g^+$ are well resolved. This vibrational level lies between closely spaced vibrational levels of the b $^1\Pi_u$ state and here a higher resolution of 40 meV was required (see inset in figure 1(*a*)). From these energy loss spectra the ratios of the

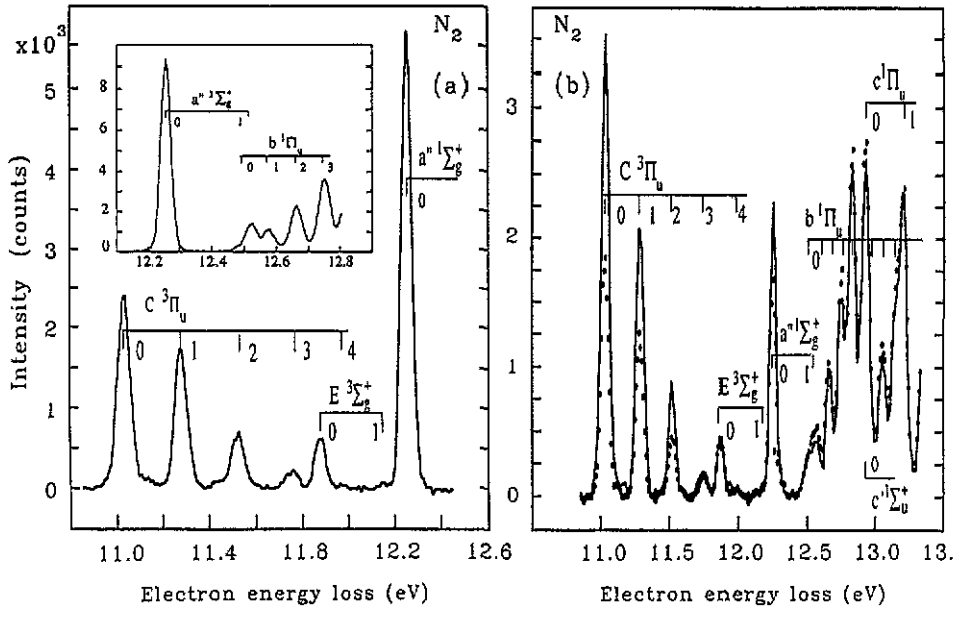

Figure 1. (*a*) Energy loss spectrum in N_2 obtained at an incident energy of 17.5 eV, an energy resolution of 60 meV and a scattering angle of 30°. The inset shows an energy loss spectrum obtained with higher resolution (40 meV) at an energy of 17.5 eV and a scattering angle of 10°. (*b*) Comparison of an energy loss spectrum (dots) obtained at an energy of 18.20 eV and a constant residual energy spectrum obtained (full curve) at a residual energy of 4.99 eV used in the determination of the transmission function of the analyser. Both spectra were measured at an angle of 30°.

inelastic cross sections for the vibrational levels of the $C\ ^3\Pi_u$, $E\ ^3\Sigma_g^+$ and $a''\ ^1\Sigma_g^+$ states with respect to that of the $v=0$ level of the $C\ ^3\Pi_u$ state were determined. This was done by comparing the peak intensities of these states in the spectra after allowance had been made for the variation in the transmission of the analyser (see section 2.3). The $v=0$ level of the $C\ ^3\Pi_u$ state was chosen as the reference as it gave rise to the largest peak in most of the spectra and also because its differential cross section changes only relatively slowly with scattering angle θ.

The differential cross section of the $v=0$ level of the $C\ ^3\Pi_u$ state was then measured against the known elastic cross section. Here, in a separate experiment, the intensity of the energy loss peak of this level was measured against that of the elastic scattering peak in the angular range 10 to 100°. The elastic intensity however was measured at a fixed incident energy of 10 eV since this corresponds to the upper limit of the range of residual energy of the inelastically scattered electrons (5.2 to 9.0 eV) for which the analyser transmission had been determined (section 2.3). This change in incident energy had a negligible effect on the electron beam profile. The ratio of the measured inelastic to elastic intensities is independent of the variation of the effective path length with scattering angle to better than 1%. This remaining small dependence is due to the different angular behaviour of the elastic and inelastic cross sections (Brinkmann and Trajmar 1981). These intensity ratios were then multiplied by the known elastic differential cross section of N_2 at 10 eV incident energy to produce the relative differential cross sections for excitation of the $C\ ^3\Pi_u$, $v=0$ level. In this normalization, the cross section of Shyn and Carignan (1980) was used. At this value of incident energy there

are two sets of data: those of Shyn and Carignan and those of Trajmar *et al* (1983), which are the renormalized results of Cartwright *et al* (1977a). Both sets of data show good agreement in their angular dependence with the Trajmar *et al* absolute values being about 10% higher.

Finally, the relative cross sections of the $C\ ^3\Pi_u$, $v=0$ level were placed on an absolute scale by normalizing to a value of 1.45×10^{-20} m^2 sr^{-1} at a scattering angle of 50° (Shyn and Carignan 1980). This normalization procedure included accurate measurements of beam current at the values of incident energy of 10, 17.5 and 20 eV and appropriate corrections of the observed scattered intensities for the transmission of the analyser. This procedure was repeated at regular intervals throughout the course of the measurements. The absolute cross sections of the remaining excited levels were deduced from the measured cross section ratios.

In the above measurements the background contributions to the intensities were determined by bypassing the gas jet and admitting the target gas directly to the vacuum chamber to produce the same base pressure which exists during measurements of scattering from the molecular beam. This procedure was especially important for scattering angles, $\theta \leqslant 20°$, where some contribution to the background due to the primary, unscattered electron beam was observed.

2.3. Calibration techniques

The transmission function of the analyser over the range of residual energy used in the present studies (5.2–10 eV) was determined in a novel way. For this, a comparison was made of an energy loss spectrum (where the incident electron energy is held fixed) and a constant residual energy spectrum (where the collection energy of the analyser is held fixed). This comparison is illustrated in figure 1(*b*). Here the incident and collection energies in the respective spectra were adjusted so that for one particular vibrational level the incident electron energy (and also the collection energy) had the same value in both spectra. The $v=1$ level of the $C\ ^1\Pi_u$ state at 13.206 eV was chosen for this purpose and it has the same intensity in both spectra of figure 1(*b*). The intensities of the peaks corresponding to other states, however, will in general be different in both spectra because they are excited at different values of incident energy and because of the difference in the transmission of the analyser at the two values of electron residual energy. This difference in the transmission was deduced from the observed intensity ratio of the $C\ ^3\Pi_u$, $v=0$ peak in the two spectra and using the recently determined excitation cross section for this state (Zubek 1994). This procedure was repeated for various values of residual energy, E_R that covered the range of 5.2 to 10 eV. The use of the integral cross section of Zubek (1994) in the procedure is justified by the observation in the present measurements that the angular distribution of the differential cross section of the $C\ ^3\Pi_u$, $v=0$ level is approximately independent of the incident energy in the range of the present studies.

The angular scale was calibrated by measuring the elastic scattering in Ar and observing the position of the minima in the differential cross sections at 15 and 20 eV in the region 60–90° (Furst *et al* 1989) and by measuring the inelastic peak intensities close to zero angle for the excitation of the $3p^5 4s\ ^1P_1$ state of Ar at 11.828 eV. This angular calibration is accurate to ±1°. The angular resolution of the measurements is estimated to be 5° and determined by the size and position of the defining aperture in the analyser and the angular divergence of the incident electron beam.

The incident electron energy was calibrated to within ±30 meV using the known position of the resonance structure of series a at 12.782 eV (Newman *et al* 1983) observed in the metastable excitation of the N_2.

2.4. Experimental uncertainties

In the calculation of the total error in the measured differential cross sections the following contributions were taken into account and are given as standard deviations:

(i) the statistical uncertainty in the intensity ratios of the energy loss peaks compared to that of the $C\,^3\Pi_u$, $v=0$ level which is estimated to be ±5%,

(ii) the statistical uncertainty in the relative $C\,^3\Pi_u$, $v=0$ cross section of ±5% for the 30–90°, ±6% for 20° and ±8% for 10 and 100°,

(iii) the statistical uncertainty in the absolute calibration at $\theta=50°$ of ±3.5% at 17.5 eV and ±4% at 20 eV,

(iv) the uncertainty in the analyser transmission calibration of ±4%,

(v) the uncertainty in the value of the elastic differential cross section of Shyn and Carignan (1980), equal to ±14%.

The total uncertainties (standard deviation) in the measured differential cross sections were taken to be equal to the square root of the sum of the square of the individual errors assuming them to be independent. These are equal to ±16% for the 20–90° angular region and ±17% for the 10 and 100° scattering angles for the $C\,^3\Pi_u$, $v=0$ cross section at both incident energies. The uncertainties in the other vibrational and the three electronic cross sections in the same angular regions are equal to ±18% and ±19% respectively.

3. Results and discussion

The ground electronic state of N_2 has the configuration: $(1\sigma_g)^2(1\sigma_u)^2(2\sigma_g)^2(2\sigma_u)^2(1\pi_g)^4(3\sigma_g)^2$. The $C\,^3\Pi_u$ valence state has the configuration $(2\sigma_u)(1\pi_u)^4(3\sigma_g)^2(1\pi_g)$ and is the upper state of the $C\,^3\Pi_u$–$B\,^3\Pi_g$ second positive system. The $E\,^3\Sigma_g^+$ and $a''\,^1\Sigma_g^+$ states are the two lowest Rydberg states being the triplet–singlet counterparts having the $X\,^2\Sigma_g^+$ ion core of N_2 and have the configuration $(2\sigma_u)^2(1\pi_u)^4(3\sigma_g)(3s\sigma_g)$. The $E\,^3\Sigma_g^+$ state is the upper state of the $E\,^3\Sigma_g^+$–$A\,^3\Sigma_u^+$ Herman–Kaplan system and the $a''\,^1\Sigma_g^+$ state is the upper state of the $a''\,^1\Sigma_g^+$–$X\,^1\Sigma_g^+$ Dressler–Lutz system (Lofthus and Krupenie 1977). The transitions from the $X\,^1\Sigma_g^+$ ground state are spin-forbidden for the $C\,^3\Pi_u$ state, spin- and symmetry-forbidden for the $E\,^3\Sigma_g^+$ state and symmetry-forbidden for the $a''\,^1\Sigma_g^+$ state.

3.1. Vibrational cross sections

The cross sections for excitation of the $v=0$ levels of the $C\,^3\Pi_u$, $E\,^3\Sigma_g^+$ and $a''\,^1\Sigma_g^+$ states, measured at 17.5 and 20 eV, are shown in figure 2 and are listed in table 1. This is the first direct determination of these vibrational cross sections. It may be seen that the angular behaviour of the $C\,^3\Pi_u$, $v=0$ cross section is different from the two other states. The ratios of the cross sections for higher levels to that of the $v=0$ level for the $C\,^3\Pi_u$ and $a''\,^1\Sigma_g^+$ states are compared with the Franck–Condon factor ratios in table 2. These are the average values for the angular range 10–100° obtained with an uncertainty (standard deviation) of 1%, 1%, 5% and 5% for the $v=1$, 2, 3 levels of the $C\,^3\Pi_u$ and $v=1$ level of the $a''\,^1\Sigma_g^+$ states respectively. The ratios for the $C\,^3\Pi_u$ state obtained

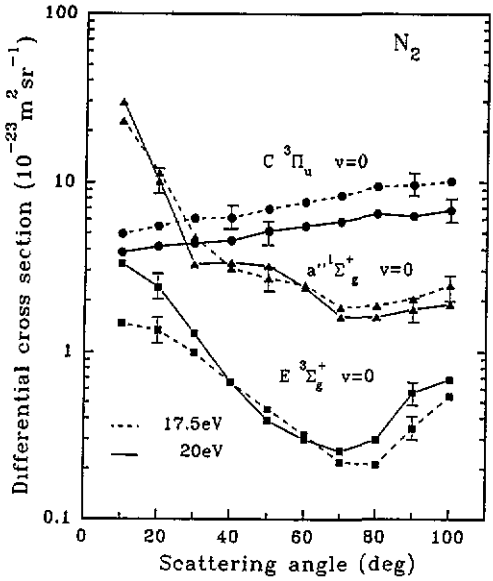

Figure 2. Differential cross sections for excitation of the $v=0$ vibrational levels of the $C\,^3\Pi_u$, $E\,^3\Sigma_g^+$ and $a''\,^1\Sigma_g^+$ states of N_2 obtained at incident energies of 17.5 and 20 eV.

Table 1. Differential cross sections in units of $10^{-23}\,m^2\,sr^{-1}$ for excitation of the $v=0$ vibrational level of the $C\,^3\Pi_u$, $E\,^3\Sigma_g^+$ and $a''\,^1\Sigma_g^+$ states of N_2 at incident electron energies of 17.5 and 20 eV.

θ	$C\,^3\Pi_u$		$E\,^3\Sigma_g^+$		$a''\,^1\Sigma_g^+$	
(deg)	17.5 eV	20 eV	17.5 eV	20 eV	17.5 eV	20 eV
10	4.94	3.84	1.47	3.30	22.9	29.8
20	5.46	4.18	1.34	2.40	11.4	10.1
30	6.09	4.35	0.992	1.29	4.72	3.27
40	6.13	4.51	0.659	0.661	3.10	3.35
50	6.93	5.14	0.451	0.386	2.71	3.20
60	7.60	5.50	0.320	0.299	2.47	2.39
70	8.32	5.85	0.220	0.255	1.83	1.61
80	9.42	6.47	0.211	0.298	1.87	1.60
90	9.59	6.28	0.348	0.568	2.05	1.78
100	10.1	6.79	0.541	0.682	2.46	1.90

at 17.5 eV are in very good agreement with those obtained in the optical emission measurements of Zubek (1994). From table 2 it can be seen that, at both incident energies the cross section ratios are larger than the ratios of the respective Franck–Condon factors. This non-Franck–Condon behaviour in the excitation of the $C\,^3\Pi_u$ state has been observed previously at higher energies above threshold (>14 eV) (Lassettre *et al* 1968, Trajmar *et al* 1970, Hirabayashi and Ichimura 1991) and more recently in the near-threshold region up to 6.5 eV above threshold (Zubek 1994).

3.2. Electronic cross sections

The electronic cross sections of the $C\,^3\Pi_u$ and $a''\,^1\Sigma_g^+$ states have been obtained by summing the vibrational cross sections within each electronic transition which have

Table 2. Relative vibrational cross sections and Franck-Condon factors (F-C) for the excitation of the $C\,^3\Pi_u$ and $a''\,^1\Sigma_g^+$ states of N_2 at incident electron energies of 17.5 and 20 eV.

	$C\,^3\Pi_u$			$a''\,^1\Sigma_g^+$		
v	17.5 eV	20 eV	F-C[a]	17.5 eV	20 eV	F-C[b]
0	1	1	1	1	1	1
1	0.620	0.666	0.558	0.130	0.176	0.067
2	0.230	0.280	0.193			
3	0.066	0.085	0.054			

[a] Lofthus and Krupenie (1977).
[b] Taken to be equal to that of $E\,^3\Sigma_g^+$ state as calculated by Cartwright (1970).

been calculated from the ratios of table 2. In this procedure allowance was made for the unobserved, higher vibrational levels. It is interesting to note that in the previous studies (Trajmar *et al* 1983, Brunger and Teubner 1990) it was assumed that the Franck-Condon principle was applicable and electronic cross sections were deduced within that approximation. For the $E\,^3\Sigma_g^+$ state the $v=1$ level has not been clearly observed in the present work and the Franck-Condon factors of Cartwright (1970) have been used in the calculations. The obtained cross sections are shown in figures 3–5 where they are compared with the results of previous studies. They are also listed in table 3.

Our $C\,^3\Pi_u$ cross section at 17.5 eV (figure 3) is in very good agreement with the results of Trajmar *et al* (1983). It confirms a slow increase of the cross section with scattering angle in the 10–100° range as is also predicted by the distorted-wave calculations of Fliflet *et al* (1979). The present result is compared to these calculations, carried

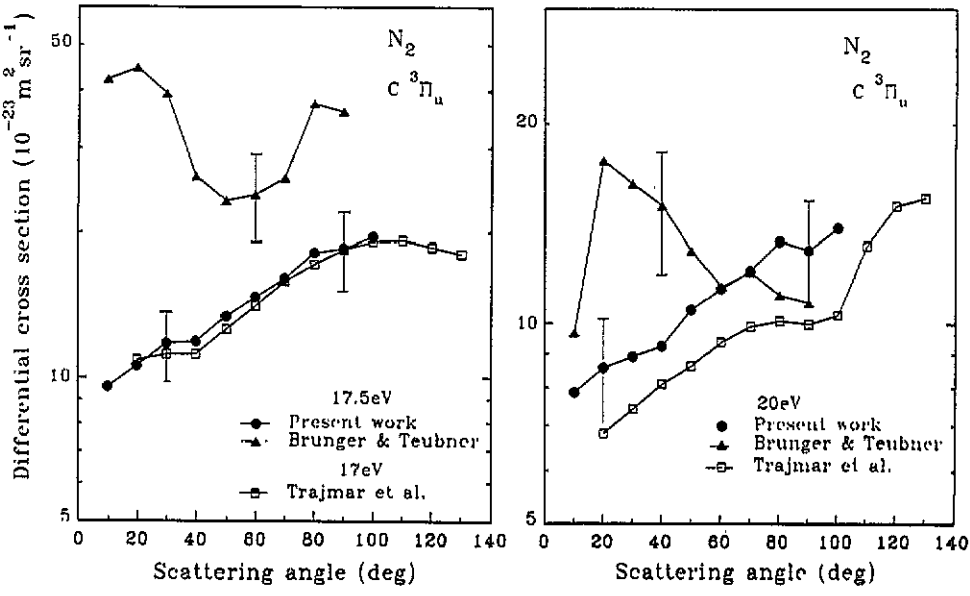

Figure 3. Differential cross sections for excitation of the $C\,^3\Pi_u$ state obtained at incident energies of 17.5 and 20 eV compared with the results of Trajmar *et al* (1983) and Brunger and Teubner (1990).

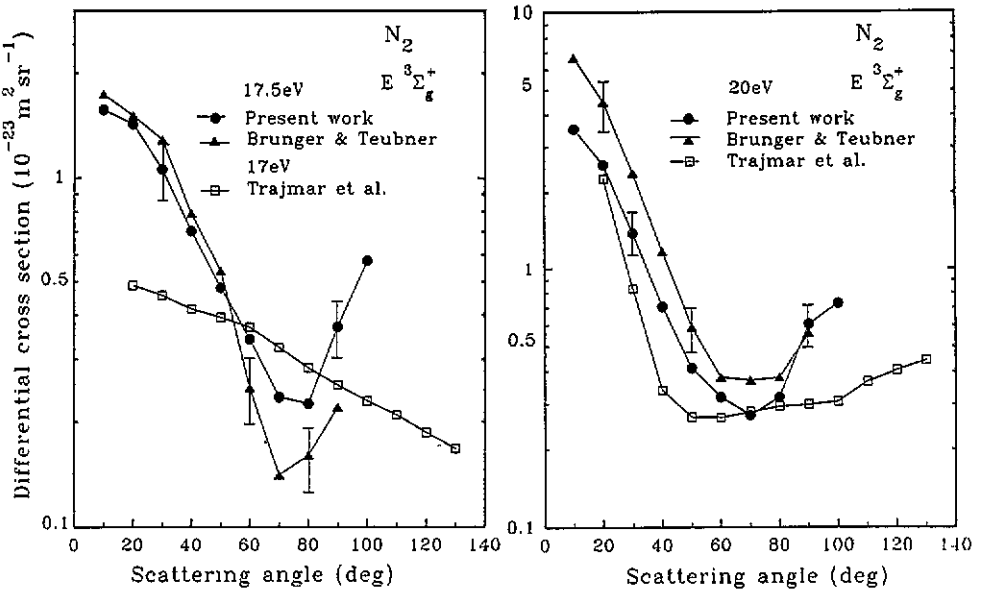

Figure 4. Differential cross sections for excitation of the $E\,^3\Sigma_g^+$ state obtained at incident energies of 17.5 and 20 eV compared with the results of Trajmar *et al* (1983) and Brunger and Teubner (1990).

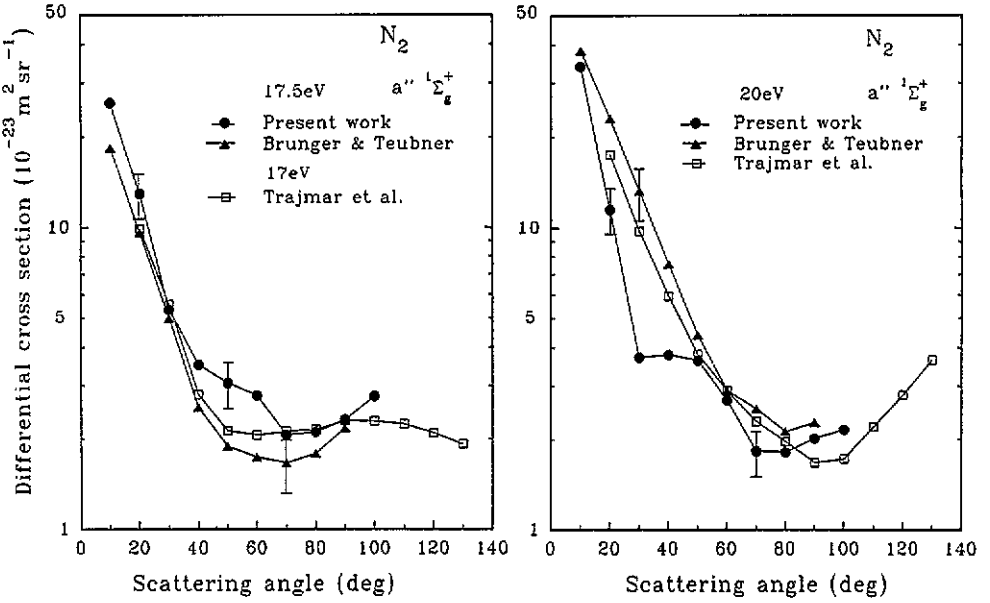

Figure 5. Differential cross sections for excitation of the $a''\,^1\Sigma_g^+$ state obtained at incident energies of 17.5 and 20 eV compared with the results of Trajmar *et al* (1983) and Brunger and Teubner (1990).

Table 3. Differential cross sections in units of 10^{-23} m^2 sr^{-1} for excitation of the C $^3\Pi_u$, E $^3\Sigma_g^+$ and a'' $^1\Sigma_g^+$ states of N_2 at incident electron energies of 17.5 and 20 eV.

θ	C $^3\Pi_u$		E $^3\Sigma_g^+$		a'' $^1\Sigma_g^+$	
(deg)	17.5 eV	20 eV	17.5 eV	20 eV	17.5 eV	20 eV
10	9.56	7.87	1.57	3.53	25.8	33.9
20	10.6	8.58	1.43	2.56	12.9	11.5
30	11.8	8.92	1.06	1.38	5.34	3.72
40	11.9	9.25	0.704	0.706	3.51	3.80
50	13.4	10.5	0.481	0.412	3.06	3.64
60	14.7	11.3	0.342	0.319	2.79	2.71
70	16.1	12.0	0.235	0.272	2.07	1.83
80	18.2	13.3	0.225	0.319	2.11	1.82
90	18.6	12.9	0.371	0.606	2.32	2.02
100	19.6	13.9	0.577	0.728	2.78	2.16

out for 17 eV incident energy, in figure 6. The calculated results are a factor of 2.3 higher but their angular dependence is in excellent agreement with our measured cross section. This is illustrated in figure 6 by the broken curve which represents the theoretical results rescaled to fit the experimental data. At 20 eV the present measurement is about 17% higher than that of Trajmar *et al* in the 20–70° region and does not reproduce a shallow minimum at about 90° observed by these authors. The results of the calculations of Fliflet *et al* (1979) for 20 eV are in less satisfactory agreement with the present cross section. The observed angular behaviour of the C $^3\Pi_u$ cross section is consistent with that typical for spin-forbidden transitions. The results of Brunger and Teubner (1990)

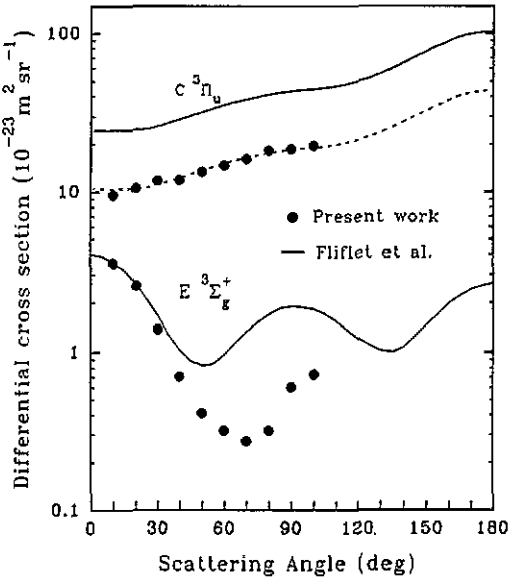

Figure 6. Comparison of the differential cross sections for excitation of the C $^3\Pi_u$ state at 17.5 eV energy and E $^3\Sigma_g^+$ state at 20 eV energy with the results of the calculations of Fliflet *et al* (1979) for 17 and 20 eV respectively. The dashed curve shows the rescaled C $^3\Pi_u$ results of the 17 eV calculations to fit the present measurements.

which are also shown in figure 3 deviate significantly from the other two sets of measured data.

Our $E\ ^3\Sigma_g^+$ cross section (figure 4) is in good agreement with the results of Brunger and Teubner (1990) for both values of incident energy and supports their observation of a minimum in the cross section at about 70°. This minimum however is not shown in the data of Trajmar *et al* although this variation of cross section has been predicted by the calculations of Fliflet *et al* (1979), which for the 20 eV energy are compared with the measured cross section in figure 6. The 17.5 eV results at 70° and 80° are the lowest cross section values measured in the present experiment and they may have a slightly higher error than quoted in section 2.4.

For the $a''\ ^1\Sigma_g^+$ state the three sets of measured differential electronic cross section (figure 5) are in relatively good agreement. However our results show more variation in the angular dependence. In particular we observe a structure at 30° in the 20 eV cross section. It is worth pointing out that our spectrometer has a better angular resolution than that used by Brunger and Teubner (12°). Also, the results of Cartwright *et al* were obtained at 20° steps which may wash out this angular variation. Our $a''\ ^1\Sigma_g^+$ cross sections show a faster decrease with scattering angle in the 10–80° range than do the $E\ ^3\Sigma_g^+$ cross sections.

3.3. Integral cross sections

Integral cross sections have been determined for electronic excitation of the $C\ ^3\Pi_u$ and $E\ ^3\Sigma_g^+$ states at incident energies of 17.5 and 20 eV. Since the present measurements were made over the angular range 10 to 100°, it was necessary to extrapolate them down to 0° and up to 180°. This was done using the theoretical cross sections of Fliflet *et al* (1979). For the $C\ ^3\Pi_u$ state it was assumed that the cross sections are described by the angular dependence of the data calculated for 17 eV. In the extrapolation of the $E\ ^3\Sigma_g^+$ cross section a second minimum at about 130° was assumed. These deduced cross sections were next integrated over the whole angular range yielding integral cross sections which are presented and compared with previous measurements in table 4. The

Table 4. Integral cross sections in units of $10^{-22}\ m^2$ for excitation of the $C\ ^3\Pi_u$ and $E\ ^3\Sigma_g^+$ states of N_2 at incident electron energies of 17, 17.5 and 20 eV.

	$C\ ^3\Pi_u$			$E\ ^3\Sigma_g^+$	
Energy (eV)	Present work	a	b	Present work	a
17.0		20.5	25.6		0.346
17.5	24.5		24.0	0.61	
20.0	18.9	14.6		0.84	0.633

[a] Trajmar *et al* (1983).
[b] Zubek (1994).

$C\ ^3\Pi_u$ cross section is in very good agreement with the measurements of Zubek (1994). The integral vibrational cross sections of the $C\ ^3\Pi_u$ and $E\ ^3\Sigma_g^+$ states can be obtained from the ratios given in table 2.

4. Conclusions

In the present work differential cross sections for electron impact excitation of the $C\ ^3\Pi_u$, $E\ ^3\Sigma_g^+$ and $a''\ ^1\Sigma_g^+$ states of N_2 have been measured at values of incident energy

of 17.5 and 20 eV and over the angular scattering range 10 to 100°. The cross sections for vibrational and electronic transitions have been obtained. These results provide additional information to help resolve discrepancies in previous cross section data for excitation of the $C\,^3\Pi_u$ and $E\,^3\Sigma_g^+$ states. Our $a''\,^1\Sigma_g^+$ cross section shows more variation with the angle than the previous studies. Using the good agreement between the present measurements and the distorted-wave calculations of Fliflet *et al* (1979) with respect to the angular behaviour the integral cross sections for the $C\,^3\Pi_u$ and $E\,^3\Sigma_g^+$ states have been also determined. For the $C\,^3\Pi_u$ state our results support the observations of Zubek (1994) and are 20% higher than the integral cross sections of Trajmar *et al* (1983). It is hoped that the results of the present measurements will stimulate further theoretical studies.

Acknowledgment

The authors gratefully acknowledge the financial support of the Science and Engineering Research Council and of the Komitet Badań Naukowych under the project 1777/2/91.

References

Brinkmann R T and Trajmar S 1981 *J. Phys. E: Sci. Instrum.* **14** 245–55
Brunger M J and Teubner P J O 1990 *Phys. Rev.* A **41** 1413–26
Brunt J N H, Read F H and King G C 1977 *J. Phys. E: Sci. Instrum.* **10** 134–9
Cartwright D C 1970 *Phys. Rev.* A **2** 1331–48
Cartwright D C, Chutjian A, Trajmar S and Williams W 1977a *Phys. Rev.* A **16** 1013–39
Cartwright D C, Trajmar S, Chutjian A and Williams W 1977b *Phys. Rev.* A **16** 1041–51
Finn T G and Doering J P 1975 *J. Chem. Phys.* **63** 4399–404
Fliflet A W, McKoy V and Rescigno T N 1979 *J. Phys. B: At. Mol. Phys.* **12** 3281–93
Furlan M, Hubin-Franskin M-J, Delwiche J and Collin J E 1990 *J. Phys. B: At. Mol. Opt. Phys.* **23** 3023–30
Furst J E, Golden D E, Mahgerefteh M, Zhou J and Mueller D 1989 *Phys. Rev.* A **40** 5592–600
Hernandez S P, Doering J P, Abreu V J and Victor G A 1983 *Planet. Space Sci.* **31** 221–33
Hirabayashi A and Ichimura A 1991 *J. Phys. Soc. Japan* **60** 862–7
Jelenković B M and Phelps A V 1987 *Phys. Rev.* A **36** 5310–26
Lassettre E N, Skerbele A, Dillon M A and Ross K J 1968 *J. Chem. Phys.* **48** 5066–96
Lofthus A and Krupenie P H 1977 *J. Phys. Chem. Ref. Data* **6** 113–228
Loureiro J and Ferreira C M 1989 *J. Phys. D: Appl. Phys.* **22** 67–75
Newman D S, Zubek M and King G C 1983 *J. Phys. B: At. Mol. Phys.* **16** 2247–63
Phelps A V and Pitchford L C 1985 *Phys. Rev.* A **31** 2932–49
Shyn T W and Carignan G R 1980 *Phys. Rev.* A **22** 923–9
Tagashira H, Taniguchi T and Sakai Y 1980 *J. Phys. D: Appl. Phys.* **13** 235–40
Trajmar S and Cartwright D C 1984 *Electron–Molecule Interactions and Their Applications* ed L G Christophorou (New York: Academic) p 155
Trajmar S, Register D F and Chutjian A 1983 *Phys. Rep.* **97** 219–356
Trajmar S, Rice J K and Kuppermann A 1970 *Adv. Chem. Phys.* **18** 15–90
Warner C D, King G C, Hammond P and Slevin J 1986 *J. Phys. B: At. Mol. Phys.* **19** 3297–303
Zubek M 1994 *J. Phys. B: At. Mol. Opt. Phys.* **27** 573–81